(2)

Ripple-Load Cracking in a Titanium Alloy

G. R. Yoder

Office of Naval Research
Arlington, VA 22217
and
P. S. Pao and R. A. Bayles

Naval Research Laboratory
Washington, DC 20375-5000

Contract No. N00014-90-WX 24009

January 1991

Scripta METALLURGICA et MATERIALIA Vol. 24, pp. 2285-2289, 1990 Printed in the U.S.A. Pergamon Press plc

RIPPLE-LOAD CRACKING IN A TITANIUM ALLOY

G.R. Yoder
Office of Naval Research
Arlington, VA 22217

and

P.S. Pao and R.A. Bayles
Naval Research Laboratory
Washington, D.C. 20375

(Received July 17, 1990)
(Revised September 20, 1990)

Introduction

The resistance of a structural material to stress-corrosion cracking is commonly assessed in terms of the threshold stress-intensity factor (K_{ISCC}) below which time-delayed fracture will not occur in an aggressive environment [1,2]. The measurement of K_{ISCC} and its application to the design of structures for the marine environment commonly presumes a sustained loading condition. Applications in the real world, however, rarely involve an absolutely constant load, but are far more apt to involve the superposition of relatively small amplitude perturbations or "ripple loads" [3,4]. (In the context of a "ripple" or small amplitude cyclic load, the stress ratio is generally presumed to be $R \geq 0.90$.) Degradation from the "ripple effect" has been expressed by Speidel as a particular concern in the case of steam turbine blade applications, for example [4]. Recent work has shown that under ripple load conditions, fracture may occur at stress-intensity levels significantly less than K_{ISCC} --- as much as 60 percent less in the case of a 5Ni-Cr-Mo-V steel; for identical loading and environmental conditions, however, no degradation was observed in the case of a 4340 steel [5]. A framework has been offered recently to predict the incidence of ripple-load degradation, approached as an extreme case of corrosion-fatigue crack growth behavior. The predicted degradations are in good agreement with observations in the case of both steels [6].

Inasmuch as titanium alloys are often employed in aggressive environments owing to their resistance to stress corrosion, it is of considerable interest to explore their sensitivity to ripple-load degradation. Since the crack tolerance properties of α/β titanium alloys can exhibit a substantial dependence on microstructural morphology, it is appropriate to examine behavior for contrasting microstructures. In the present study, a Ti-6Al-4V alloy is examined for two microstructures that have been observed to affect fracture toughness, fatigue and corrosion-fatigue crack growth resistance [7-9], viz. a Widmänstatten colony type microstructure --- as developed from a beta anneal (BA), versus an equiaxed primary α-phase morphology generated from a recrystallization anneal (RA).

Materials and Experimental Procedures

The Ti-6Al-4V alloy studied was received in the form of an α/β rolled plate with the composition (in wt pct): Ti-6.7Al-4.3V, 0.10Fe, 0.20O, 0.03C, 0.011N and 0.006H. Details of subsequent heat treatments used to generate the different microstructures are given in Table I together with the resultant mechanical properties.

Measurements of corrosion-fatigue crack growth rates (da/dN) and K_{ISCC} threshold were made in 3.5% aqueous NaCl solution (circulating) from precracked WOL-type compact tension specimens of 25.4 mm thickness, TL crack orientation, half-height to width ratio of 0.486. Crack length was determined from a compliance related CMOD technique [10]. To simulate a ripple-load condition, specimens were cyclically loaded with a stress ratio (minimum stress: maximum stress), R=0.90, --- as illustrated schematically in Fig. 1, a haversine waveform and a frequency of υ = 5Hz. With statically loaded samples to assess K_{ISCC}, loads were sustained at constant levels for periods of ~ 100 h, sufficient to establish thresholds with titanium alloys [2].

0036-9/48/90 $3.00 + .00

Results and Analysis

The "window" for ripple-load cracking susceptibility [6] is established by an upper bound equal to the static K_{ISCC} threshold and a lower bound threshold for ripple-load cracking given by $K^{RL}_{max}\big|_{th} = \Delta K_{th}/(1-R)$ where ΔK_{th} is the threshold for corrosion-fatigue crack growth as illustrated in Fig. 2. Values of ΔK_{th} and K_{ISCC} as measured for both the Widmänstatten and equiaxed microstructures are displayed in Table II, and the associated corrosion-fatigue crack growth rate curve in Fig. 3. Accordingly, the window for ripple-load cracking susceptibility is exhibited for each microstructure in Fig. 4. Clearly, the potential for degradation by ripple load effects is much larger for the Widmänstatten microstructure - with a ripple load threshold 53% less than the static threshold K_{ISCC}, as compared to only a marginal degradation of ~ 9% in the case of the equiaxed microstructure. It is also of more than passing interest to observe here that the material/microstructure with the greater K_{ISCC} resistance is found to exhibit the greater sensitivity (susceptibility) to ripple-load degradation; a similar finding was made in prior work with ferrous alloys [5,6]. Moreover, the Ti-6Al-4V microstructure with the inferior K_{ISCC} threshold, viz. the equiaxed primary α-phase microstructure, actually exhibits a ripple-load threshold in excess of that for the Widmänstatten microstructure. Such behavior underscores the importance of considering ripple-load cracking sensitivity in the selection of structural materials for real world application in the marine environment, as opposed to consideration solely on the basis of static K_{ISCC} threshold.

Also, it should be pointed out that time-to-failure (t_f) can be predicted from the corrosion-fatigue crack growth rate data for a given structural geometry according to [6]:

$$t_f = \frac{1}{\upsilon} \sum_j \int_{\{a_i\}_j}^{\{a_f\}_j} \frac{da}{C_j \left| (1-R) P_{max} f(a,Q) \right|^{m_j}}$$

where P is load, f (a,Q) is a function of crack length (a) and structural geometry (Q) which together with (a) define a stress-intensity factor, and C_j and m_j are fatigue crack growth rate power-law constants for the j segment of a piecewise integration. If this is done for the specimen geometry employed in this study, using the corrosion-fatigue data in Fig. 3, the t_f predictions are shown by the dotted (solid circle) trend lines displayed within the windows of Fig. 4. Direct experimental confirmation of the trend lines for the Widmänstatten microstructure is indicated with a pair of data points (open circle), with t_f measured under ripple-load conditions.

Conclusions

1. Under ripple-load conditions, fracture of Ti-6Al-4V alloy can occur in salt water at levels of stress-intensity factor much less than the threshold for stress-corrosion cracking, K_{ISCC}.
2. Such ripple-load degradation in cracking resistance appears to be microstructurally dependent, with a Widmänstatten colony microstructure exhibiting a ripple-load cracking threshold to less than 50 percent of K_{ISCC} in contrast to a marginal degradation of only 9 percent observed for an equiaxed primary alpha-phase morphology.
3. As observed in prior work with ferrous alloys, the material/microstructure with the greater K_{ISCC} resistance was found to exhibit the greater sensitivity to ripple-load degradation; in fact, the Ti-6Al-4V/microstructure with the lesser K_{ISCC} threshold actually exhibits the greater threshold for ripple-load cracking.

Acknowledgments

The support of this work by the Office of Naval Research is gratefully acknowledged, as is the encouragement of Dr. A. J. Sedriks, ONR Scientific Officer.

References

1. B.F. Brown, Stress-Corrosion Cracking in High Strength Steels and in Titanium and Aluminum Alloys, p. 27, U.S. Government Printing Office, Washington (1972).
2. R.W. Judy, Jr. and R.J. Goode, Stress Corrosion - New Approaches, STP 610, p. 72, ASTM, Philadelphia(1976).
3. K. Endo, K. Komai, and N. Himejima, Trans. Japan Soc. Mech. Engrs. 37, 2036(1971).

4. M.O. Speidel, Corrosion Fatigue of Steam Turbine Blade Materials, p.1-1, Pergamon, New York (1983).
5. T.W. Crooker, J.A. Hauser II and R.A. Bayles, Environmental Degradation of Engineering Materials, p. 521, Pennsylvania State University Press, University Park (1987).
6. P.S. Pao, R.A. Bayles and G.R. Yoder, Trans. ASME, J. Eng. Matls Tech., Series H, in press (1990).
7. G.R. Yoder, L.A. Cooley and T.W. Crooker, Metall. Trans. A. 8A, 1737 (1977).
8. G.R. Yoder, L.A. Cooley and T.W. Crooker, Trans. ASME, J. Eng. Matls Tech., Series H 99, 313 (1977).
9. G.R. Yoder, L.A. Cooley and T.W. Crooker, Corrosion Fatigue: Mechanics, Metallurgy, Electrochemistry and Engineering STP 801, p. 159, ASTM, Philadelphia (1983).
10. G.R. Yoder, L.A. Cooley, and T.W. Crooker, Fatigue Crack Growth Measurement and Data Analysis, STP 738, p. 85, ASTM, Philadelphia(1981).

Table I Heat Treatments and Mechanical Properties

Heat Treatments

Recrystallization Anneal (RA)	954°C 4h; HC @ 180°C/h to 760°C; HC @ 370°C/h to 480°C; AC
Beta Anneal (BA)	1038°C 0.5h; HC to RT + 732°C 2h; HC

(HC = helium purge and cool, AC = air cool, RT = room temperature)

Mechanical Properties

Heat Treatment	Yield Strength (MPa)	Tensile Strength (MPa)	% elongation
RA	931	1007	15
BA	869	958	16

Table II Predicted and Measured Threshold Values (MPa$\sqrt{m}$)

Heat Treatment	K_{ISCC}	$K^{RL}_{max}\|_{th}$
RA	42.7	39
BA	60	28

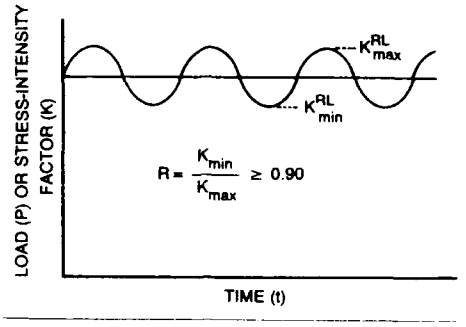

Fig. 1 Schematics of a "ripple" load superposed on larger sustained load.

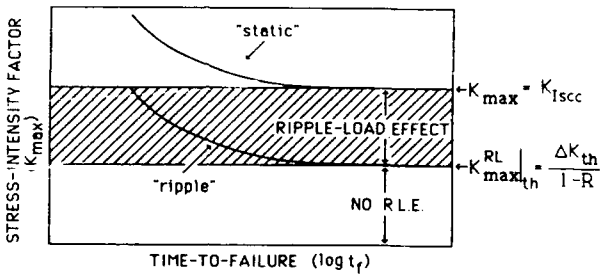

Fig. 2 Illustration of ripple-load effect and its predictions.

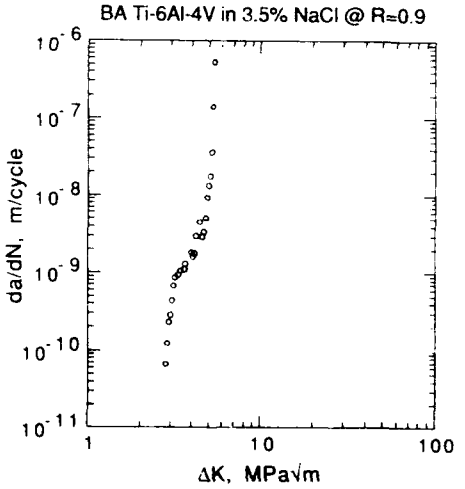

Fig. 3 Fatigue crack growth rate of beta-annealed Ti 6Al 4V in 3.5% NaCl solution @ R=0.9.

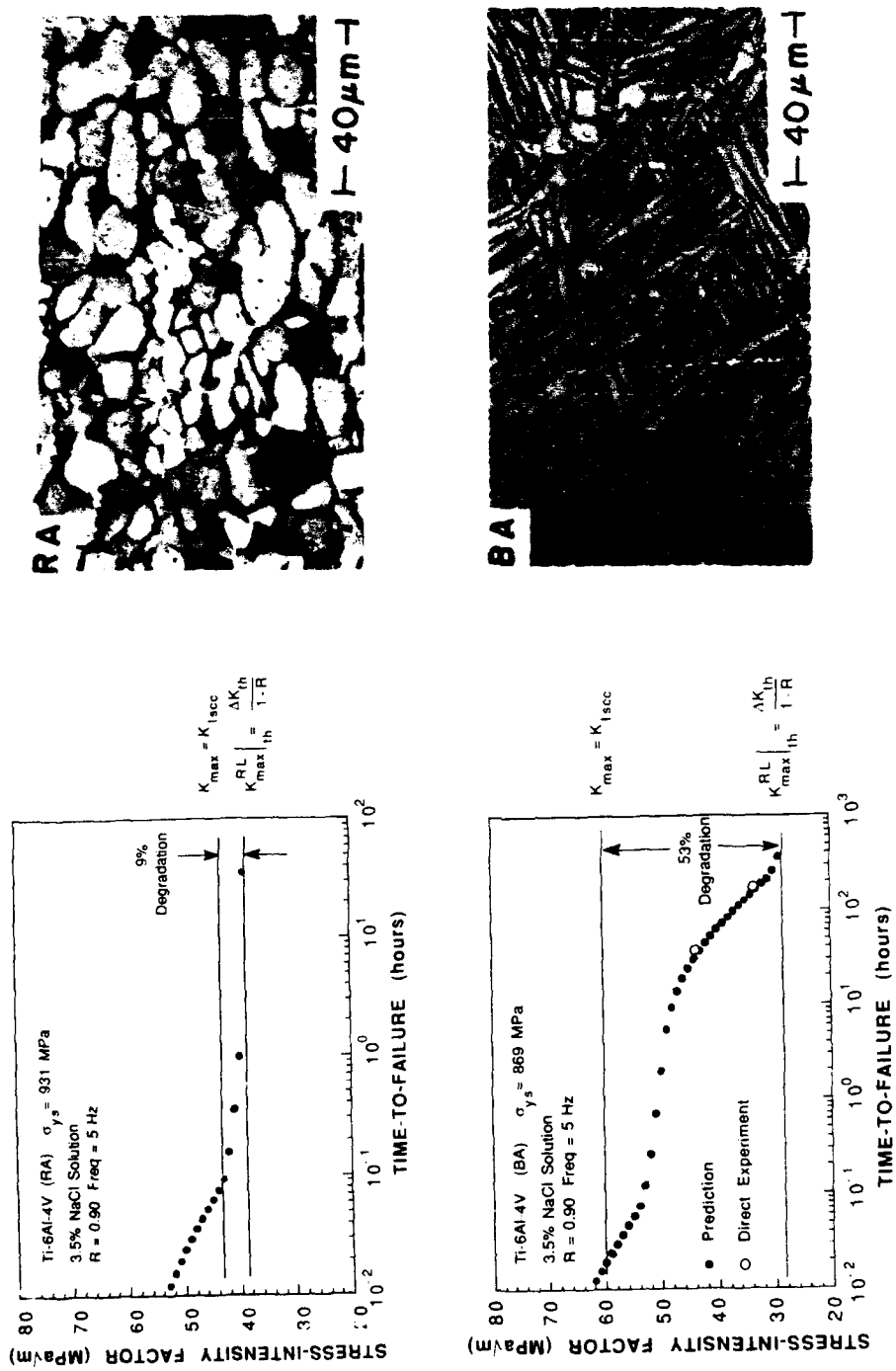

Fig. 4 Comparison of ripple-load degradation in beta-annealed and recrystallization-annealed Ti-6Al-4V.